REAL-TIME ATTITUDE DETERMINATION OF A NANOSATELLITE USING GPS SIGNAL-TO-NOISE RATIO OBSERVATIONS

SHAUN M. STEWART and GREG N. HOLT

The Department of Aerospace Engineering and Engineering Mechanics
The University of Texas at Austin

Advising Professor: DR. E. GLENN LIGHTSEY

Abstract- In support of the FASTRAC nanosatellite mission, a COTS, single antenna GPS receiver has been augmented for use in space as a multi-purpose navigation sensor. In addition to providing measurements of position and velocity, the Mitel Orion GPS receiver has been coupled with a three-axis magnetometer to provide robust attitude determination for the FASTRAC nanosatellite pair. An algorithm is presented for attitude determination of small spacecraft using single antenna GPS signal-to-noise ratio observations coupled with a magnetometer. Real-time accuracies of 5-7 degrees RMS are demonstrated in simulation. In addition, a benchmark testing procedure for evaluating the on-orbit performance of the receiver is presented. The procedure is used to characterize the raw measurement accuracy and systematic tracking loop errors for the Orion receiver. An on-orbit demonstration of the integrated sensor is planned for 2006. The integrated device is intended as a low-cost, standard solution for use on small spacecraft. Algorithm and hardware simulation results are provided to show the usefulness, accuracy, and robustness of this approach.

INTRODUCTION

The utilization of Global Positioning System (GPS) signal-to-noise ratio measurements (SNR) from a single antenna receiver is an innovative approach for attitude determination of LEO spacecraft. For spacecraft that are orbiting below the GPS constellation, GPS sensors have proven to be a low cost solution for orbit determination. In addition to requirements on position and velocity, most spacecraft have pointing requirements necessary for completion of their mission objectives. For instance, proper orientation of spacecraft solar arrays with respect to the sun, of cameras or other instruments with respect to objects of interest, and of directional antennas toward communication centers are all often critical for mission success. Presented here is a method for combining GPS with a three-axis magnetometer (TAM) in order to provide relatively accurate and robust attitude solutions. A least-squares extended Kalman filter (EKF) algorithm has been utilized to estimate the attitude of the spacecraft in quaternion form. After each measurement update, the spacecraft attitude quaternion is then transformed into roll, pitch, and yaw angles, and both the quaternion and Euler angles are reported for use by the attitude control system.

This algorithm was initially utilized to process GPS signal-to-noise ratios (SNR) in tandem with GPS differential carrier phase measurements between multiple antennas [1]. However, the present algorithm has been modified to support a single antenna SNR solution coupled with a magnetometer for use on small spacecraft. Because this algorithm requires only a single GPS antenna, the spacecraft surface area requirements as well as the GPS hardware complexity are greatly reduced. Magnetometers alone can be used to determine the attitude of low-Earth orbiting spacecraft. However, the measurements supply only a single vector point of reference. Thus, attitude solutions can only be computed after a sufficient amount of motion through the Earth's magnetic field has occurred. The combination with GPS signal-to-noise ratio measurements has eliminated this requirement.

A combined GPS and magnetometer attitude determination setup would be attractive where space is at a premium and it is not possible to utilize an array of GPS antennas, such as on a nanosatellite. A GPS receiver is generally required for such a satellite to determine position, velocity, and time. In addition, the SNR measurements, when coupled with a magnetometer, can also provide low cost, light weight, and power efficient way to determine the attitude of the vehicle.

The objective of this work is to provide a proof-of-concept demonstration for the determination of the attitude of a small spacecraft using GPS signal-to-noise ratio measurements coupled with a magnetometer. Off-the-shelf GPS hardware was used to demonstrate the feasibility of the GPS attitude determination algorithm for this problem. An on-orbit demonstration will be implemented on The University of Texas FASTRAC nanosatellite mission planned for launch in 2006.

The objective of the FASTRAC mission is to investigate technologies that enable space research using satellite formations. The utilization of satellite formations in space is a pivotal advancement for the future of space exploration and research. In addition to demonstrating the integrated GPS/TAM attitude sensor as an innovative enabling technology for satellite formations, the FASTRAC team has developed an innovative benchmark test for characterizing COTS GPS receiver performance on-orbit. The test is used to demonstrate the raw measurement accuracy and tracking loop performance for the Orion receiver after completion of firmware modifications enabling its use in space.

This paper is organized as follows. First, a discussion of the GPS SNR attitude estimation algorithm is presented. The measurement models for GPS signal-to-noise ratio and three-axis magnetometers are reviewed, and a quaternion representation for spacecraft attitude, a dynamic model, and key EKF equations are presented for use with the combined GPS/TAM attitude sensor. Then, a description of the benchmark testing procedure and analysis are presented. Finally, the testing setup and results for the GPS Orion receiver benchmark testing and algorithm simulation are provided.

SNR MEASUREMENT MODEL

An estimate of the orientation of an antenna can be obtained by measuring the signal-to-noise ratio of incoming GPS signals and comparing them against the antenna gain pattern, which is known in the body frame. Generally, multiple receiver antennas are required to determine full three-axis attitude. However, a single GPS antenna when coupled with a magnetometer can also be used to observe full 3-axis attitude.

This method was first explored by Axelrad and Behre to generate single pointing vector solutions [2]. Dunn and Duncan used a similar technique to obtain point vector solutions that were accurate to within 15 degrees on the Microlab-1 satellite [3]. Full three-axis attitude solutions were computed by Buist, et al [4] using a single antenna on a gravity gradient stabilized satellite known as PoSAT-1. In this case, the presence of a gravity gradient boom created variation in the azimuthal gain pattern of the antenna which was combined with the gravity gradient dynamics to generate solutions that agreed to within 10 degrees of those derived independently using a magnetometer.

Full attitude solutions from a single GPS antenna are generally not possible, however, since the gain pattern of a hemispherical antenna typically has little or no variation in the azimuth direction and the knowledge of the vehicle dynamics may be limited. The SNR approach was further developed by Lightsey and Madsen [5] to provide full three-axis solutions by utilizing multiple antennas with non-parallel boresight vectors. This approach demonstrated that three-axis root mean square (RMS) errors of approximately 3 degrees are possible in simulation [1].

The orientation of a GPS receiver antenna can be described by a single unit vector, $\hat{A}$, fixed at the center of the antenna, normal to the surface. This vector is called the antenna boresight vector. Because the receiving antenna's gain pattern is approximately known and invariant in the body frame, it is possible to derive the antenna boresight vector orientation from incoming GPS signal-to-noise ratio measurements. The strength of incoming GPS signals are attenuated as a function of the angle between the GPS line-of-sight vector, $\hat{L}$, and the antenna boresight vector.

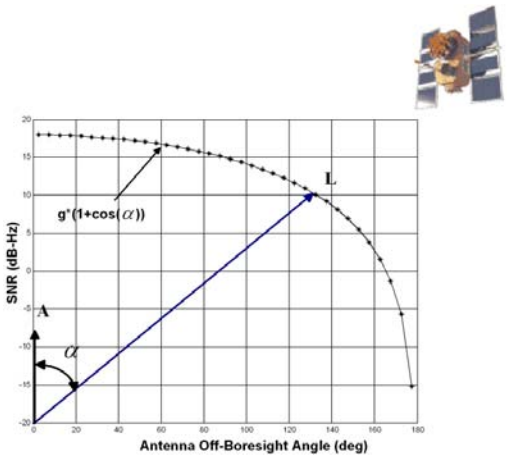

Figure 1: Off-boresight Angle.

A hypothetical model for the signal attenuation can be approximately described as a cosine function:

$$\mathrm{SNR} \approx g * (1 + \cos(\alpha)) \quad (1)$$

where

g is the antenna gain.

α is the incident angle of incoming GPS signals.

Given that this attenuation function is approximately known, it can be used to relate the antenna gain with the incident angle of incoming GPS signals [1]. The dot product between the antenna boresight vector and the GPS line-of-sight vector gives a scalar relationship for the angle between them, α.

$$\hat{A} \cdot \hat{L} = \cos(\alpha) = A_x L_x + A_y L_y + A_z L_z \quad (2)$$

where

$\hat{A}$ is the antenna boresight vector.

$\hat{L}$ is the normalized LOS vector to the GPS satellite.

α is the angle between $\hat{A}$ and $\hat{L}$.

The scalar relationships described in equations 1 and 2 provide a basis for estimating the orientation of the antenna boresight vector with respect to the GPS constellation. Figure 1 describes the orientation of the antenna boresight vector with respect to the GPS line-of-sight vectors. Using a precise model of the antenna attenuation function and a minimum of three incoming GPS signal-to-noise ratio measurements, the off-boresight angle, α, corresponding to each visible GPS satellite can be used to derive an estimate of the orientation of the body-fixed antenna boresight vector [2][4].

QUATERNION ATTITUDE

A useful method for representing attitude is with the vector axis of rotation ($\underline{u}$) and the angle of rotation (γ) about that axis. An efficient way of representing this information is with a quaternion. A useful property of quaternions is that they are not susceptible to singularity and uniqueness problems as is the case with Euler angles. This is of particular concern with the spacecraft attitude problem due to the wide range of motion that is possible.

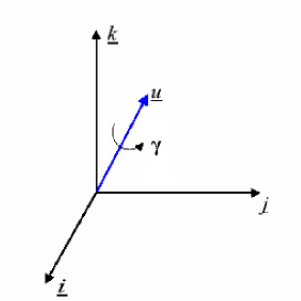

Figure 2: Quaternion Vector and Angle.

For this reason, they are numerically a more stable representation for rotations. The quaternion is represented in the following manner:

$$q = q_0 + \hat{i}q_1 + \hat{j}q_2 + \hat{k}q_3 \quad (3)$$

To describe a rotation, the quaternion can be thought of as having a scalar part and a vector part:

$$q_0 = \cos(\gamma/2) \quad (4)$$

$$\underline{q} = \underline{u}\sin(\gamma/2) \quad (5)$$

$$q = q_0 + \underline{q} \quad (6)$$

where the norm of q is one.

The quaternion is an efficient way to describe the attitude and the quaternion rates are well suited to numerical integration. As such, it is the preferred method for representing the attitude of spacecraft. As a drawback, however, the quaternion is not simple to visualize. The quaternion may however be transformed into the standard roll (ϕ), pitch (θ), and yaw (ψ) angles corresponding to the 1-2-3 Euler angle sequence through the following formulas.

$$\phi = \tan^{-1}\left(\frac{2(q_2q_3 + q_0q_1)}{2q_0^2 + 2q_3^2 - 1}\right) \quad (7)$$

$$\theta = \sin^{-1}(-2q_1q_3 - 2q_0q_2) \quad (8)$$

$$\psi = \tan^{-1}\left(\frac{2(q_1q_2 + q_0q_3)}{2q_0^2 + 2q_1^2 - 1}\right) \quad (9)$$

The attitude determination problem can be viewed as one of determining the rotation that a set of body vectors has gone through to move it from its nominal orientation to its current orientation. When the body goes through such a

rotation, each vector on the body also goes through that same rotation. If the body frame has been chosen such that it is aligned with the external reference frame during nominal conditions, then the rotated antenna boresight vector, $\hat{A}_{rot}$, can be expressed as a function of the attitude state and the unrotated boresight vector. The unrotated antenna boresight vector is aligned along the zenith vector and thus denoted as $\hat{A}_k$. Using the quaternion multiplication, the quaternion point rotation between the spacecraft's nominal and current attitude is given as:

$$\hat{A}_{rot} = (2q_0^2 - 1)\hat{A}_k + 2(\underline{q} \cdot \hat{A}_k)\underline{q} + 2q_0(\hat{A}_k \times \underline{q}) \quad (10)$$

where

$$\underline{q} = \begin{bmatrix} q_1 \\ q_2 \\ q_3 \end{bmatrix} \quad (11)$$

It may be desirable to define the body axes such that they do not coincide with the attitude body frame during nominal operation. For example, in order to simplify the dynamic equations, principal axes were assumed. In all likelihood the principal axes will not happen to align with the attitude body frame. If this is the case, the actual attitude is then the estimated quaternion multiplied by the known bias quaternion. The measurement model is the same as before, and is repeated here for clarity.

$$G_1 = \hat{A}_{rot} \cdot \hat{L} = \cos(\alpha) = A_x L_x + A_y L_y + A_z L_z \quad (12)$$

The additional observation of the Earth's magnetic field direction is processed in conjunction with the GPS signal-to-noise ratio measurements in an Extended Kalman Filter. The simultaneous processing of GPS SNR and magnetometer measurements allows for estimation of the full three-axis attitude of the spacecraft.

THREE-AXIS MAGNETOMER MODEL

Magnetometers are another type of attitude sensor widely used on spacecraft. These sensors operate by estimating both the direction and magnitude of the local magnetic field. They are reliable, lightweight, and have low power requirements. They can operate over a wide range of temperatures and they have no moving parts. A three-axis magnetometer measures the Earth's magnetic field direction and magnitude in the spacecraft body coordinates. This measurement is then compared to a model of the Earth's magnetic field. The difference between these two is a function of the vehicle attitude. This situation is traditionally represented as:

$$\underline{B}_b = R\underline{B}_0 + \underline{\varepsilon} \quad (13)$$

where

$\underline{B}_b$ is the magnetic field measurement in the body frame.

R is the rotation from the nominal frame to the body frame.

$\underline{B}_0$ is the known magnetic field vector in the nominal frame.

$\underline{\varepsilon}$ is assumed to be a zero-mean Gaussian measurement error with a std. dev. of 0.3 mG.

The problem of estimating the vehicle rotation from magnetometer observations is very similar to the GPS SNR problem and is actually simpler than the algorithm that has already been presented. In the GPS SNR algorithm, it was necessary to derive a relationship between the reported measurement and the antenna boresight vector. In this instance, however, the vector of interest is observed directly as the magnetic field strength recorded by the magnetometer. Hence no intermediate relation is needed to map the measurement to the physical phenomena being observed. The measurement model is simply the expected magnetic field vector. The rotation which aligns the magnetic field model with the measured magnetic field strength will also rotate the spacecraft from the nominal frame to its current body frame. A quaternion frame rotation is used to relate the magnetic field model referenced in the external frame to the three-axis magnetometer measurement made in the body frame. The quaternion representation for the required rotation is given by:

$$\underline{b}_{rot} = (2q_0^2 - 1)\underline{b}_m + 2(\underline{q} \cdot \underline{b}_m)\underline{q} + 2q_0(\underline{q} \times \underline{b}_m) \quad (14)$$

where

$\underline{b}_m$ is the modeled magnetic field strength.

q is the current estimate for the rotation.

$\underline{b}_{rot}$ is the rotation from the nominal to body frame.

DYNAMIC MODEL

The most dominant effect on the vehicle attitude in space is modeled by Euler's equations. These equations predict how a rigid body's attitude will change through time in the presence of external torques. If principal axes are used, the equations may be expressed as follows:

$$\begin{aligned}\dot{\omega}_x &= \frac{1}{I_x}\left[\left(I_y - I_z\right)\omega_y\omega_z + T_x\right] \\ \dot{\omega}_y &= \frac{1}{I_y}\left[\left(I_z - I_x\right)\omega_x\omega_z + T_y\right] \\ \dot{\omega}_z &= \frac{1}{I_z}\left[\left(I_x - I_y\right)\omega_x\omega_y + T_z\right]\end{aligned} \tag{15}$$

where

T_i is the sum of external torques on the $\hat{i}^{th}$ body axis.

I_x, I_y, and I_z are the principal moments of inertia.

ω_x, ω_y, and ω_z are the vehicle body rates.

These equations are valid when expressed in an inertial reference frame. The local vertical local horizontal (LVLH) reference frame, in which the spacecraft attitude is expressed, is a non inertial frame due to the orbital motion. Euler's equations may be modified to account for this difference. The resulting equations are:

$$\begin{aligned}\dot{\omega}_x &= \frac{1}{I_x}\left[\left(I_y - I_z\right)\omega_y\omega_z + T_x\right] + \omega_0\omega_z \\ \dot{\omega}_y &= \frac{1}{I_y}\left[\left(I_z - I_x\right)\omega_x\omega_z + T_y\right] \\ \dot{\omega}_z &= \frac{1}{I_z}\left[\left(I_x - I_y\right)\omega_x\omega_y + T_z\right] - \omega_0\omega_x\end{aligned} \tag{16}$$

where ω_0 is the mean motion.

For some applications, external torques may be neglected and the algorithm may still provide the necessary accuracy. For other applications, however, it is important to model the external torques in more detail. The application of these external torques is vehicle and orbit dependent. Therefore, no external torques were modeled for the tests of the algorithm.

ATTITUDE DETERMINATION

The state, *X*, for the EKF algorithm is defined as the quaternion rotation from the nominal frame to the current body frame. In addition to the quaternion, the vehicle body rates are also included in the state. This allows the quaternion to be propagated through time and allows for the dynamic modeling of the vehicle attitude.

$$X = \begin{bmatrix} q_0 \\ q_1 \\ q_2 \\ q_3 \\ \omega_x \\ \omega_y \\ \omega_z \end{bmatrix} = \begin{bmatrix} x_1 \\ x_2 \\ x_3 \\ x_4 \\ x_5 \\ x_6 \\ x_7 \end{bmatrix} \tag{17}$$

The equations of motion for the system are then defined by the time rate of change of the state. Integration of these equations will allow for modeling of the changes in the vehicle state in between measurement updates. The partial of these equations with respect to the state is defined as the A matrix.

$$\dot{X} = F(X,t) = \begin{bmatrix} \dot{q} \\ \dot{\omega} \end{bmatrix} \tag{18}$$

$$A \equiv \left.\frac{\partial F(X,t)}{\partial X}\right|_* = \left[\begin{matrix} A_{11} & A_{12} \\ 0 & A_{22} \end{matrix}\right]_* \tag{19}$$

where

$$A_{11} = \left[\begin{matrix} 0 & -\omega_x & -\omega_y & \omega_z \\ \omega_x & 0 & \omega_x & -\omega_x \\ \omega_y & \omega_z & 0 & \omega_x \\ \omega_z & \omega_y & -\omega_x & 0 \end{matrix}\right]_*$$

$$A_{12} = \left[\begin{matrix} -q_1 & -q_2 & -q_3 \\ q_0 & -q_3 & q_2 \\ q_3 & q_0 & -q_1 \\ -q_2 & q_1 & q_0 \end{matrix}\right]_*$$

$$A_{22} = \left[\begin{matrix} 0 & \frac{1}{I_x}\left(I_y - I_z\right)\omega_z & \frac{1}{I_x}\left(I_y - I_z\right)\omega_y + \omega_0 \\ \frac{1}{I_y}\left(I_z - I_x\right)\omega_z & 0 & \frac{1}{I_y}\left(I_z - I_x\right)\omega_x \\ \frac{1}{I_z}\left(I_x - I_y\right)\omega_y - \omega_0 & \frac{1}{I_z}\left(I_x - I_y\right)\omega_x & 0 \end{matrix}\right]_*$$

The A matrix is evaluated using the current estimate, denoted by '*', and used to propagate the covariance, P, to the current measurement epoch.

$$\dot{P} = AP + PA^T + Q \tag{20}$$

Here, a process noise matrix, Q, is also utilized to ensure a lower bound for the measurement covariance and to prevent the estimator from becoming insensitive to measured changes is vehicle attitude. The observation matrix, H, is used to map the current state into the measurement model. Each row of the H matrix, denoted $\widetilde{H}$, maps a scalar measurement into its corresponding measurement model. Since there are two different sensors being used for the attitude estimate, two different $\widetilde{H}$ matrices must be used for the GPS and magnetometer measurements respectively. Referring to equations 2 and 14, the two measurement models are given by:

$$G_1 = \hat{A} \cdot \hat{L} = \cos(\alpha) = A_x L_x + A_y L_y + A_z L_z \tag{21}$$

$$G_2 = \underline{b}_{rot}$$

$$G_2 = (2q_0^2 - 1)\underline{b}_m + 2(\underline{q} \cdot \underline{b}_m)\underline{q} + 2q_0(\underline{q} \times \underline{b}_m) \tag{22}$$

Taking the partial derivatives of these equations with respect to the state give the rows of the $\widetilde{H}$ vectors. These vectors are then stacked into a single H matrix which is used to process all the measurements for the current epoch and update the estimate for the state.

$$H = \begin{bmatrix} \widetilde{H}_{\text{GPS1}} \\ \vdots \\ \widetilde{H}_{\text{GPS12}} \\ \widetilde{H}_{\text{Mag1}} \\ \vdots \\ \widetilde{H}_{\text{Mag3}} \end{bmatrix}_{*[15x3]} \tag{23}$$

Unique $\widetilde{H}$ vectors are required for the GPS signal-to-noise ratio measurements as well as each component of the magnetometer measurement. Essentially, each reported component of the measured magnetic field vector is treated as an individual scalar measurement, and processed accordingly. These equations are greatly simplified by aligning the nominal antenna boresight direction with the body z-axis:

$$\widetilde{H}^T_{\text{GPS}} = -2 \begin{bmatrix} -x_3 & x_2 & 2x_1 \\ x_4 & x_1 & 0 \\ -x_1 & x_4 & 0 \\ x_2 & x_3 & 2x_4 \\ 0 & 0 & 0 \\ 0 & 0 & 0 \\ 0 & 0 & 0 \end{bmatrix} \cdot \begin{bmatrix} L_x \\ L_y \\ L_z \end{bmatrix} \tag{24}$$

$$\widetilde{H}^T_{\text{Mag1}} = 2 \begin{bmatrix} 2x_1 b_{m1} + x_3 b_{m3} - x_4 b_{m2} \\ 2x_2 b_{m1} + x_3 b_{m2} + x_4 b_{m3} \\ x_2 b_{m2} + x_1 b_{m3} \\ x_2 b_{m3} - x_1 b_{m2} \\ 0 \\ 0 \\ 0 \end{bmatrix} \tag{25}$$

$$\widetilde{H}^T_{\text{Mag2}} = 2 \begin{bmatrix} 2x_1 b_{m2} + x_4 b_{m1} - x_2 b_{m3} \\ x_3 b_{m1} - x_1 b_{m3} \\ 2x_3 b_{m2} + x_2 b_{m1} + x_4 b_{m3} \\ x_3 b_{m3} + x_1 b_{m1} \\ 0 \\ 0 \\ 0 \end{bmatrix} \tag{26}$$

$$\widetilde{H}^T_{\text{Mag1}} = 2 \begin{bmatrix} 2x_1 b_{m3} + x_2 b_{m2} - x_3 b_{m1} \\ x_4 b_{m1} + x_1 b_{m2} \\ x_4 b_{m2} - x_1 b_{m1} \\ 2x_4 b_{m3} + x_2 b_{m1} + x_3 b_{m2} \\ 0 \\ 0 \\ 0 \end{bmatrix} \tag{27}$$

BENCHMARK TESTING

Receiver performance may be defined on many levels, most obviously the final processed navigation solution. This solution, however, is heavily dependent on the estimation and filtering of the raw measurements and will vary by

application. More fundamentally, the receiver performance may be characterized by raw measurement accuracy and systematic tracking loop errors. These low-level performance measurements are common to the entire GPS architecture and are the focus of this study. Any navigation algorithm written for a particular application will be fundamentally limited by the accuracy of the raw measurements from the receiver. In addition, evaluating the raw measurement performance is useful to understand and optimize the low-level receiver software. For the FASTRAC mission, GPS benchmark testing was used to improve the tracking loop code and evaluate performance of individually fabricated receiver boards.

In order to provide full insight into the characteristics of the tracking loops and measurement collection, all errors must be preserved, isolated, and reported in the analysis. For this reason it is necessary to perform the raw measurement and tracking loop evaluations on a GPS constellation simulator. Although a stationary outdoor antenna is much less expensive and more accessible for most testers, it has several drawbacks when compared to a simulator. The constellation simulator is able to provide a realistic high Doppler environment which affects the raw measurements in space but is not seen in a ground test. The simulator is also able to provide an environment free from external errors such as satellite ephemeris errors, satellite clock errors, ionosphere and troposphere effects, and multipath. Any errors seen in the simulation tests are primarily due to the receiver hardware and tracking loops. Simulators are also able to create repeatable test conditions which lead to verifiable results.

Test Configuration

The constellation simulator used for this research is shown in Figure 3. It is a Spirent (formerly Global Simulation Systems) model STR4760 and has 2 dual-frequency output ports with 16 channels per port. Complete simulator specifications may be found in the manual by Spirent [6]. The simulator is controlled by a Digital Electronics Corporation (DEC) Alpha Workstation shown in Figure 3. It is manufactured by Compaq, Inc. and uses the Open Virtual Memory System (Open VMS) operating system. A complete description of the orbital simulation scenario is found in Holt [7]. The scenario is summarized below:

Figure 3: Spirent GPS Constellation Simulator (left) and DEC Alpha Open VMS Workstation (right).

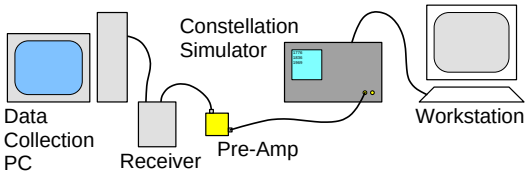

Figure 4: Laboratory Simulation Equipment.

- Semi-major Axis: 6823.0 km
- Eccentricity: 0.001
- Inclination: 87^{o}
- Longitude of Ascending Node: 135^{o}
- Argument of Perigee: 0^{o}
- Mean Anomaly: 0^{o}
- Epoch: 6 Nov 2001 00:00.00 GPS, 5 Nov 2001 23:59:57 UTC
- GPS Week: 1139, 172800 seconds

The orbital simulation is for a low earth satellite in a near polar orbit. The almanac file used to generate this scenario was YUMA1139. All environmental and ephemeris errors were eliminated from this scenario. These include ionosphere, troposphere, multipath, satellite clock, and satellite ephemeris errors. For this experiment the components were set up in the configuration of Figure 4. The standard orbital test was initiated on the simulator during each data run. The signal was sent through a preamplifier and then to the receiver under evaluation, with the signal gain adjusted for the noise environment of the simulator. The data output stream was collected on a computer via a serial connection. The receivers were tested for two hours in this environment. This time span was sufficient to give multiple horizon-to-horizon GPS visibility arcs for differencing.

GPS Receiver

The Orion receiver used on FASTRAC is based on a published design by Zarlink using the Plessey chipset. The engineering model was built and the source code was refined at The University of Texas at Austin Center for Space Research. The Orion receiver was originally designed for terrestrial applications as a single frequency, 12 channel, single RF design. Source code modifications have made the receiver capable of outputting code, carrier, Doppler offset, carrier-smoothed code, and carrier-derived range rate measurements. This source code has internal time tag synchronization to integer seconds based on GPS Time when position fixing. The firmware used in this test uses a second order FLL-aided PLL for its tracking loop. The Orion receiver has flown in space aboard the student-designed experimental PCSat with preliminarily good results [8]. Detailed Orion receiver descriptions may be found in the technical report by Montenbruck, et. al [9].

ANALYSIS

The analysis for this research is designed to produce performance results for low-level receiver measurements. Specifically, the analysis seeks to isolate raw measurement accuracy and systematic tracking loop errors. In a GPS measurement, however, the dominant features are the geometric quantities and oscillator errors. This research uses the technique of interchannel differencing to remove these errors. While Kaplan [10] mentions how this method has been used many times in relative positioning, its use in receiver performance analysis is a new development. In previous studies of raw measurement accuracy, curve fitting has been used to remove these errors [11]. While curve-fitting method does show the "white-noise" characteristics of the measurement, it has the disadvantage of masking any systematic errors in the receiver. These errors can identify otherwise undetected dynamic filter problems. By using differencing instead of curve-fitting, this study seeks to remove only the geometric and oscillator dependent errors and preserve the white-noise and systematic errors of the receiver. To effectively use this methodology, certain assumptions were made.

Assumptions

Some assumptions are made in the analysis to simplify the tests and processing. The main assumption concerns the reference truth measurements from the GPS constellation simulator. In a perfect test, the signal that is generated by the simulator is exactly what is output in the reference file. Since this is never entirely true, the results of the measurement differencing will actually give a combination of error from the receiver channels *and* the simulator. It is assumed for this procedure that the simulator error is negligible compared to the receiver error.

In addition, simulator truth estimates are collected at 1 second intervals and interpolated for when output measurements do not line up with integer seconds. It is assumed that interpolation errors are negligible with respect to the measurements under analysis. To validate this, the simulated orbit is considered. For this scenario, the mean motion is approximately 1 $mrad/s$ with accelerations $\approx 8\,m/s^2$, acceleration rates $\approx 20\,mm/s^3$, and fourth-order rates $\approx 0.013\,mm/s^4$. A piecewise cubic Hermite polynomial interpolation method was used for which the error is well documented [11]**.** The error is represented as:

$$\varepsilon(x) = f(x) - h_{2m-1}(x) = \psi_m(x)^2 \frac{f^{2m}(\xi)}{(2m)!} \quad (28)$$

where

$$\psi_m = \prod_{j=0}^{m} (x - x_j) \quad (29)$$

$$f^k(\xi) = k^{th} \text{ deriv. of } f \text{ evaluated at } \xi$$

and m=2 for a cubic Hermite polynomial.
By selecting the nearest time interval so that the interpolation is always less than 0.5 seconds, the neglected term represents less than $4 \times 10^{-5}\,mm$, which is many orders of magnitude smaller than the most accurate carrier phase measurement in the test.

Finally, the simulated signal levels are assumed to be the actual signal levels experienced in an orbital environment. This is important because tracking loop performance can be directly affected by low signal-to-noise ratio (SNR). While simulated signal levels will vary with preamplifier and front-end selection, a common power level was selected as +8 dB

above the nominal GPS signal level. The power increase is detailed as follows:

- +3 dB: Average antenna gain
- +3 dB: GPS signal level higher than published
- +2 dB: Thermal noise floor is higher in electronic simulator than in real environment – need higher signal level to maintain same SNR

This power level gives SNR readings in most receivers which are similar to live-sky tests.

Differencing

Figure 5 shows the analysis technique used for the tests. As stated before, the dominant features of a receiver measurement are the geometric distance (range) and speed (range rate) between the receiver and GPS satellite.

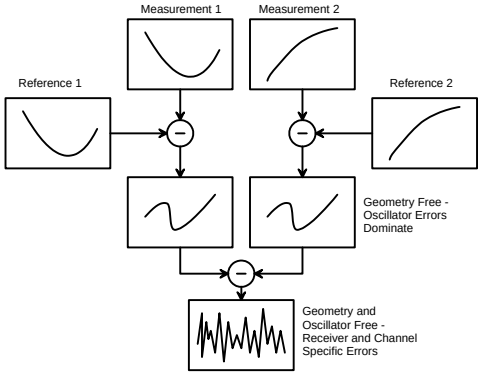

Figure 5: Measurement Differencing Technique.

The first step in the data analysis is to subtract the simulated, reference geometric quantities from the measurement to give an "error from truth" representation. This is analogous to the classic GPS "receiver-receiver" single-difference technique except the simulated reference is used as one of the "receivers." The quantity that results is free from common-mode satellite errors and is dominated by receiver oscillator drifts and other errors. This procedure is performed for two GPS measurements at a time when their visibility overlaps. Mathematically, the receiver measurement, Meas_i, consists of range, ρ_i, oscillator errors, δT, and other receiver errors, ε_i.

$$\text{Meas}_i = \rho_i + \delta T + \varepsilon_i \tag{30}$$

The simulator reference, Ref_i, consists of range, ρ_i, and simulator errors, ε_{Si}.

$$\text{Ref}_i = \rho_i + \varepsilon_{Si} \tag{31}$$

These are subtracted to give the single difference, SD_i.

$$\begin{aligned} \text{SD}_i &= \text{Meas}_i - \text{Ref}_i \\ &= \delta T + \varepsilon_i + \varepsilon_{Si} \end{aligned} \tag{32}$$

The next step in the analysis is to difference the results of the previous operations on two different measurements taken at the same time. This removes common oscillator errors and the remaining quantity represents receiver and channel specific errors. This is analogous to the classic GPS double-difference except the result is not a baseline between two receivers but an error measurement of a single receiver. This result is the double difference, DD_{1-2}.

$$\begin{aligned} \text{DD}_{1-2} &= \text{SD}_1 - \text{SD}_2 \\ &= +\varepsilon_1 - \varepsilon_2 + \varepsilon_{S1} - \varepsilon_{S2} \end{aligned} \tag{33}$$

As stated previously, it is assumed the last two terms (simulator errors) are negligible with respect to the first two (receiver/channel specific errors). If the errors are independent and have equal standard deviation, the resulting Root Mean Square (RMS) error will be scaled by $\sqrt{2}$ since a double difference was used. For these independent errors, the receiver intrinsic accuracy, $\text{Acc}(\varepsilon)$, is related to the measured error, ε_{meas}, as discussed in Yates [12]:

$$\begin{aligned} \text{Acc}(\varepsilon_{meas}) &= \sqrt{\frac{1}{n}\sum_{i=1}^{n}\varepsilon_i^2} \\ \text{RMS}(\varepsilon_{meas}) &= \sqrt{\frac{1}{n}\sum_{i=1}^{n}2\varepsilon_i^2} \\ &= \sqrt{2}\,\text{Acc}(\varepsilon_{meas}) \end{aligned} \tag{34}$$

The reported accuracy will be a mean value of all errors from both channels and the simulator.

Data Arc Selection

Receiver performance may be characterized in terms of application specific parameters (e.g., multipath) and application independent parameters (e.g., tracking loop error). In order to create a general measurement of receiver performance, application independent parameters were evaluated. These parameters are believed to be functions of signal dynamics (Doppler shift) and signal strength (SNR).

Table 1: Dynamics and Signal Level Conditions.

PRN 1	PRN 2	Start Time (sec)	End Time (sec)	Max. Signal Level (dB)	Max. Relative Accel. (g's)
2	28	174000	175800	10	0.1
14	29	178100	180000	9	0.2
3	15	177400	178900	8	0.3
21	28	173900	174700	9	0.9
13	22	176500	177700	9	1.0
6	17	177100	178000	7	0.8

To examine receiver performance in a variety of conditions, six data arcs were selected from the simulation as standardized time intervals. Since satellite selection algorithms vary from receiver to receiver, no guarantee exists that a receiver will track both satellites during a particular test interval. With six test intervals, however, the receiver will provide usable data for at least some of the intervals.

Figure 6: Sample GPS Satellite Arc for Test Scenario.

Figure 6 shows and example GPS satellite data arc generated from GPS Orion receiver observations. The arc in blue shows the received signal strength (SNR) of the incoming GPS signal in decibels (dB). The red arc describes the elevation of the GPS satellite. Note the correlation between these two arcs, which is primarily attributed to the receiver antenna gain pattern.

These data arcs contain a variety of relative dynamics and signal level conditions. This is important because, as discussed, the raw measurement accuracy is affected by these two factors. The relative dynamics conditions come from the differential velocity and acceleration of the two GPS satellites. Satellites with similar rise/set profiles will have low relative dynamics whereas satellites with differing rise/set profiles will have high relative dynamics. The highest relative dynamics will occur when one SV is just rising (or setting) as the other reaches the peak of its arc. The highest signal levels will occur when both satellites have high elevations at the same time. Table 1 summarizes the relative dynamics and signal level conditions for the standardized test intervals. Figure 6 shows sample rise/set profiles for the GPS satellites visible in the simulation. These plots were used to select the standard test intervals based on common satellite visibility and line-of-sight (LOS) acceleration.

BENCHMARK TESTING RESULTS

The receiver was tested with a modified version of `DLR16707H' developed by the German Space Operations Center (GSOC). The pseudorange output is smoothing capable, but for this test only code-based pseudorange was considered. The entire range of tests was performed, and an interesting case is presented here. In early tests with this receiver, a systematic trend was found in the carrier phase measurements. The same trend was found in another version of the receiver, so a hardware disparity issue was ruled out. This trend is shown in Figure 7, with the original in red and the corrected in blue. The trend appears to be proportional to the LOS accelerations shown in Table 1, a result consistent with the use of the second order PLL found in the Orion. This information was used in code debugging to internally correct the carrier phase measurements for acceleration dependence by numerically estimating the acceleration. A third order PLL is also under development to remove the acceleration.

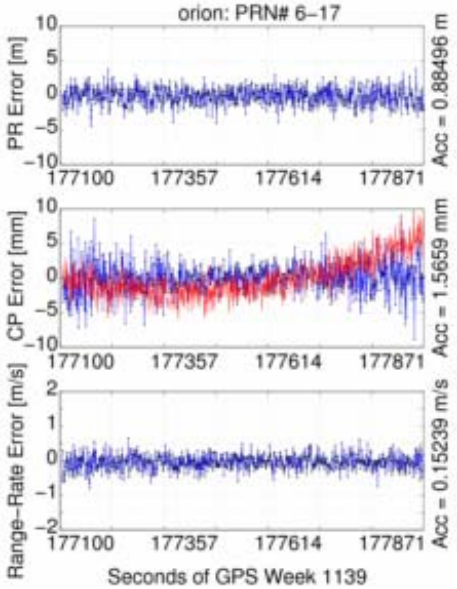

Figure 7: Orion Systematic Acceleration Dependence Before (red) and After (blue) Tracking Loop Modifications.

It is significant to note that only this differencing test could identify a systematic trend and allow for the relatively simple correction.

With the corrected code it is clear that the Orion receiver in this test configuration has no systematic errors in pseudorange, carrier phase, or range rate measurements. The noise is in an expected range for unsmoothed values of pseudorange and range rate.

ATTITUDE SIMULATION SETUP

After the benchmark testing was completed, a hardware simulation of the combined GPS/Magnetometer attitude estimation approach was conducted to demonstrate the achievable on-orbit performance of the algorithm using the COTS GPS Orion receiver. A STR 4760 Spirent Communications Multi-Satellite GPS Navigation Simulator was used to generate the GPS RF signal for a LEO orbit. The GPS simulator allows for modeling of a receiver antenna's gain pattern as well as the vehicle dynamics. A single antenna, Orion GPS receiver was used to record the spacecraft position and velocity, the LOS vectors for each visible GPS satellite, and the SNR corresponding to each satellite signal.

In order to simulate on-orbit magnetic field measurements, the International Geomagnetic Reference Field (IGRF) model was used.

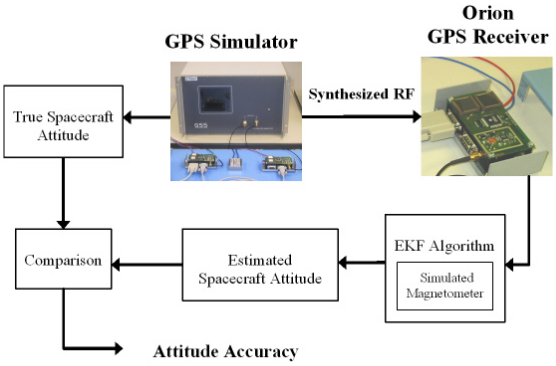

Figure 8: Attitude Simulation Setup.

While magnetometer measurements are known to be very accurate, the errors associated with the model of the Earth's magnetic field are typically an order of magnitude larger than and are also nonlinear and orbit dependent in nature [13]. In order to model this type of behavior, the `true' magnetic field was modeled using a $10^{th}$ order IGRF with coefficients from the year 2000. The `measurements' were simulated by using a 6^{th} order IGRF model with coefficients from 1995 and by adding a zero mean white noise Gaussian process with a standard deviation of 0.3 mG. This simulation approach was previously utilized by Crassidis and Lightsey and is typically used to simulate magnetometer sensor errors [14].

The attitude determination algorithm was implemented in post processing using the SNR measurements provided by the Orion receiver. The accuracy of the processed attitude results were characterized by comparing them against the true vehicle dynamics generated by the simulator.

ATTITUDE SIMULATION RESULTS

The GPS raw measurements were processed at 1-Hz during a 140-minute simulation for a slowly tumbling satellite. The processed measurements (position, velocity, LOS, and SNR) were gathered and post-processed in the EKF attitude estimation algorithm. Figure 9 shows the true and estimated roll, pitch, and yaw angles for the spacecraft during the ~2-hour simulation. Note that the variation in yaw is primarily due to the motion of the LVLH frame with respect to the body frame as the satellite completes an orbit. This is a once per orbit variation.

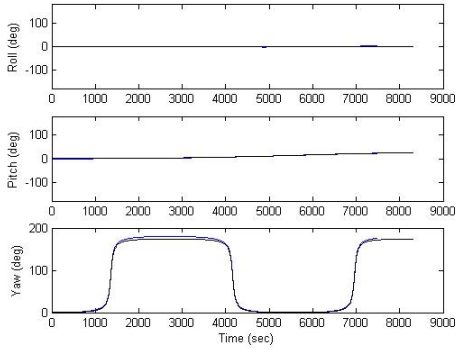

Figure 9: True and Estimated Attitude.

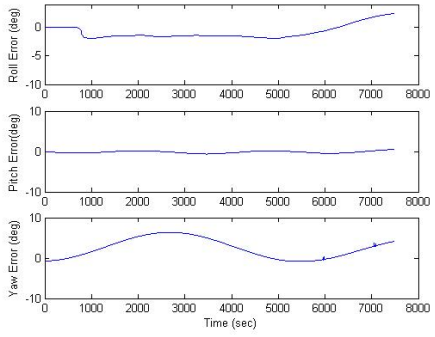

Figure 10: Estimator Performance vs. Time.

Figure 10 shows that the estimated vehicle roll, pitch, and yaw angles are kept within 10 degrees of the true attitude. During the entire simulation the estimator maintained an accuracy of ± 5 degrees RMS.

These results demonstrate that the combined GPS-TAM sensor can generate robust attitude estimates. Immediately after acquisition of the GPS signal, the estimator was able to generate an accurate estimate for the vehicle attitude accurate to within 5 degrees. Investigations are ongoing to characterize the performance of the algorithm given an inaccurate apriori estimate, and for increased vehicle tumble rates.

CONCLUSION

In this paper, magnetometer measurements were combined with observations from a single antenna GPS receiver to provide robust three-axis attitude estimates for a LEO spacecraft. It was demonstrated that an RMS accuracy of ~5 degrees is achievable using commercial off-the-shelf hardware. Given that this level accuracy is attainable using COTS hardware, performance greater than 5 degrees may be achieved given the utilization of a more accurate GPS receiver.

In support of the FASTRAC nanosatellite mission, the firmware of the Orion GPS receiver has been augmented for use in space as a multi-purpose navigation sensor. In addition, a benchmark test was presented as a standard method for characterizing GPS receiver performance. The procedure was used to characterize the raw measurement accuracy and systematic tracking loop errors for the Orion GPS receiver during and after its firmware modifications. It was shown that the receiver in its current test configuration has no systematic errors in pseudorange, carrier phase, or range rate measurements. An on-orbit demonstration of the integrated GPS/TAM sensor is planned for 2006.

REFERENCES

[1] Madsen, J.D., "Robust Spacecraft Attitude Determination Using Global Positioning System Receivers," PhD Dissertation, The University of Texas at Austin, May 2003.

[2] Axelrad, P. and Behre, C.P., "Satellite Attitude Determination Based on GPS Signal-to-Noise Ratio," *Proceedings of the IEEE*, vol. 87, no. 1, pp. 133-144, January 1999.

[3] Dunn, C. and Duncan, C., "Estimating Attitude From GPS Measurements on One Antenna," NASA Tech Brief, June 1998.

[4] Buist, P.J. et al., "Spacecraft Full Attitude Determination from a Single Antenna: Experimentation with the PoSAT-1 GPS Receiver," *ION Technical Meeting*, pp. 181-1817, September 1998.

[5] Lightsey, E.G. and Madsen, J.D., "Three-Axis Attitude Determination Using Global Positioning System Signal Strength Measurements," *AIAA Journal of Guidance, Control and Dynamics*, vol 26, no. 2, pp. 304-310, March-April 2003.

[6] "STR Series Multichannel Satellite Navigation Simulators Reference Manual," Tech. Rep. DGP00032AAC, Spirent Comm., Ltd., Devon, UK, 2001.

[7] Holt, G. "GPS Receiver Benchmark Testing," Tech. Rep., The University of Texas Center for Space Research, Austin, TX, 2002.

[8] Montenbruck, O, et. al. "GPS Operations on the PCSat Microsatellite," *ION GPS*, Sept 2002.

[9] Montenbruck, O., M. Markgraf, and S. Leung, "Space Adaptation of the GPS Orion Firmware," Tech. Rep. DLR/GSOC TN 01-08, Oberpfaffenhofen, November 2001.

[10] Kaplan, E., ed., *Understanding GPS Principles and Applications*, Artech House, Boston, 1996.

[11] Ryan, S., et. al., "DGPS Kinematic Carrier Phase Signal Simulation Analysis in the Velocity Domain," *ION GPS Conference*, Sept 1997.

[12] Yates, T., D. Goodman, *Probability and Stochastic Processes*, John Wiley and Sons, New York, 1999.

[13] J. L. Crassidis et al. Contingency Designs for Attitude Determination of TRMM. Flight Mechanics Estimation Theory Symposium, pages 419-433, May 1995.

[14] J. L. Crassidis and E. G. Lightsey. Attitude Determination Using Combined GPS and Three-Axis Magnetometer Data. Proceedings International Workshop on GPS, January 2000.